This is a preprint, the final version is subject to change, of the American Mineralogist (MSA)
Cite as Authors (Year) Title. American Mineralogist, in press.
(DOI will not work until issue is live.) DOI: http://dx.doi.org/10.2138/am.2014.4588

CORRECTED MANUSCRIPT 20/10/2013

A calorimetric and thermodynamic investigation of the synthetic analogues of cobaltomenite, $CoSeO_3 \cdot 2H_2O$, and ahlfeldite, $NiSeO_3 \cdot 2H_2O$.

Marina V. Charykova[1], Vladimir G. Krivovichev[1*],
Maksim I. Lelet[2], Oxana S. Yakovenko[1],
Evgeny V.Suleimanov[2], Wulf Depmeier[3],
Viktorina V. Semenova[1], and Maina L. Zorina[1]

[1]Department of Geology, St. Petersburg State University, 7–9 University Embankment, Saint-Petersburg 199034, Russia.
[2]Department of Chemistry, Nizhny Novgorod State UniversityNizhny, 65 Ilyinskaya St., Novgorod, 603950, Russia.
[3]Institut für Geowissenschaften – Abt. Mineralogie-Kristallographie, Universität Kiel, Olshausenstraße 40, D-24098 Kiel, Germany.

*Corresponding author. E-mail: vkrivovi@yandex.com

Abstract

Thermophysical and thermochemical calorimetric investigations were carried out on synthetic analogs of two minerals: cobaltomenite ($CoSeO_3 \cdot 2H_2O$) and ahlfeldite ($NiSeO_3 \cdot 2H_2O$). The synthesis was realized by mixing of aqueous solutions of cobalt and nikel nitrates, accordingly, and sodium selenite, acidified with the help of a solution of nitric acid and characterized by XRD powder diffraction and FTIR spectroscopy methods. The low-temperature heat capacity of $CoSeO_3 \cdot 2H_2O$ and $NiSeO_3 \cdot 2H_2O$ were measured using adiabatic calorimetry between 8 and 340 K, and the third-law entropies were determined. Values of S^o(298 K, $CoSeO_3 \cdot 2H_2O$, cr.) = 183.2 ± 1.0 J/(mol·K) and S^o (298 K, $NiSeO_3 \cdot 2H_2O$, cr.) = 172.9 ± 1.0 J/(mol·K) are obtained with an uncertainty of 0.5%. The enthalpies of formation for $CoSeO_3 \cdot 2H_2O$ and $NiSeO_3 \cdot 2H_2O$ were determined by solution calorimetry with H_2SO_4 solution as the solvent and giving $\Delta_f H^o$(298 K, $CoSeO_3 \cdot 2H_2O$, cr.) = –1135.3 kJ/mol, $\Delta_f H^o$(298 K, $NiSeO_3 \cdot 2H_2O$, cr.) = –1133.3 kJ/mol. The Gibbs energy of formation for $CoSeO_3 \cdot 2H_2O$ and $NiSeO_3 \cdot 2H_2O$ at T = 298 K, 1 atm can be

calculated on the basis on $\Delta_f H^o$ and $\Delta_f S^o$: $\Delta_f G^o$ (298 K, $CoSeO_3 \cdot 2H_2O$, cr.) = –937.4 kJ/mol and $\Delta_f G^o$ (298 K, $NiSeO_3 \cdot 2H_2O$, cr.) = –932.4 kJ/mol. Smoothed Cp°(T) values between T = 0 K and T = 320 K for $CoSeO_3 \cdot 2H_2O$ (cr.) and $NiSeO_3 \cdot 2H_2O$ (cr.) are presented along with values for S° and the functions [H°(T)-H°(0)] and [G°(T)-H°(0)]. These results motivate a re-evaluation of the natural conditions under which selenites, and selenates replace selenides, and sulfides in the oxidation zones of sulfide ore deposits or upon weathering of technologic waste. The values of $\Delta_f G°$ for $CoSeO_3 \cdot 2H_2O$ and $NiSeO_3 \cdot 2H_2O$ were used to calculate the Eh–pH diagrams of the Co–Se–H_2O and Ni–Se–H_2O systems. These diagrams have been constructed for the average contents of these elements in acidic waters of the oxidation zones of sulfide deposits. The behavior of selenium, cobalt, and nickel in the surface environment have been quantitatively explained by variations of the redox potential and the acidity–basicity of the mineral-forming medium. Precisely these parameters determine the migration ability of selenium compounds and its precipitation in the form of various solid phases.

Keywords: cobaltomenite, ahlfeldite, heat capacity, entropy, enthalpy of formation, the Gibbs energy of formation.

Introduction

Since the discovery of the toxic properties and biological significance of selenium, there have been continuous studies of the geological occurrence and geochemistry of this element in oxygenated aqueous environments. Drainage from mineralized and mined areas may have high concentrations of dissolved selenium, and this is of major concern as waterflows, soils and plants in the vicinity of ore bodies containing Se-bearing sulfides and selenides are prone to be the low-temperature oxidizing environments for the natural sources of Se (Treatise on Geochemistry 2004). Most selenites are formed by chemical weathering of ores by oxygenated waters establishing conditions of increased Eh and low or neutral pH (with seasonal fluctuations of temperatures and atmospheric pressure). These parameters define the migration of selenium, and its precipitation in the form of selenite minerals (chalcomenite $CuSeO_3 \cdot 2H_2O$, cobaltomenite $CoSeO_3 \cdot 2H_2O$, ahlfeldite $NiSeO_3 \cdot 2H_2O$, mandarinoite $Fe_2(SeO_3)_3 \cdot 6H_2O$, molybdomenite $PbSeO_3$). Eh–pH diagrams of the Me–Se–H_2O systems (Me = Co, Ni, Fe, Cu, Zn, Pb) have been published, which make it possible to estimate the conditions for the near-surface formation of Se minerals (selenites) (Krivovichev et al. 2011).

The analysis of the thermodynamic data for calculation of mineral equilibria involving selenites and selenates of Fe, Cu, Zn, Pb, Co, and Ni (Seby et al. 2001; Olin et al. 2005; Charykova et al. 2010) showed that, even in cases when it is possible to find corresponding parameters in the literature, they frequently raise questions and need specification. In particular, this is true for the standard thermodynamic functions of ahlfeldite, $NiSeO_3 \cdot 2H_2O$, and cobaltomenite, $CoSeO_3 \cdot 2H_2O$. Their standard enthalpies were determined by Selivanova et al. (1963; 1964), and then with use of data from Thukhlantsev, and Tomashevsky (1957) the standard entropy and Gibbs energy of their formation were calculated. These experimental data have been used for the calculation of standard thermodynamic functions of ahlfeldite and cobaltomenite, cited in many reference books and data bases (Vlaev et al. 2005).

Ahlfeldite and cobaltomenite are rare minerals, which are formed only in the oxidation zone of sulfide- and selenide-bearing ores in the deposits Serro-de-Kacheuta (Argentina), Pahakake, Dragon (Bolivia), Muzoni (Zaire), and some hydrothermal deposits in the State of Utah (USA). The experimental determination of thermodynamic data of rare minerals in general, and of the title compounds in particular, on the basis of studying their solubility or by calorimetric measurements can hardly rely on natural samples, because they usually do not occur in sufficient amounts, form only tiny crystals, may include inclusions, be covered by weathering crusts, and almost inevitably contain impurities. All these defects influence many properties of the samples studied and certainly their thermodynamic parameters. In this communication we therefore present the results of our

investigations of the enthalpy of formation and of the heat capacity of synthetic analogues of cobaltomenite and ahlfeldite.

Experimental methods

Sample preparation.

For the synthesis of cobalt and nickel selenites we have used a modification of a technique proposed in Vlaev et al. (2005; 2006). The synthesis was realized by boiling-dry of aqueous solutions of cobalt and nickel nitrates, respectively, and sodium selenite, acidified with a solution of nitric acid. To the warm (50^{o}C) 0,2N solution of nickel or cobalt salts (pH 5.2-5.3) a 0,2N solution of Na_2SeO_3 (pH 6.0-6.2) was added slowly and dropwise. After heating for 2-3 hours and hashing for a weak solution with the residue have been left to ripen at room temperature for 20 days, after which the formed precipitate was separated by decantation**,** washed with distilled water and dried at room temperature.

The phase purity of the synthetic products was characterized using an XRD powder diffractometer (Rigaku Miniflex II) and a FTIR spectrometer BRUKER VERTEX 80. Its composition was determined using X-ray fluorescence (dual-beam system operating with a scanning focused ion beam and a scanning electron beam Quanta 200 3D FEI). In addition, the concentrations of Co, Ni, Se in the synthesized phases were determined (after their full dissolution in acidic solutions) by means of method ICP MS (mass spectrometer ELAN-DRC-e, PERKIN ELMER).

Calorimetric methods

The enthalpies of formation for $CoSeO_3{\cdot}2H_2O$ and $NiSeO_3{\cdot}2H_2O$ were determined using solution calorimetry with H_2SO_4 solution as the solvent. The heat of solution was measured using a differential heat-conducting Tian-Calvet calorimeter Calvet 2.0 (Lelet et al. 2011) T = 298 K. Dissolution experiments were performed in a Teflon container holding a smaller inner-Teflon vessel. The inner vessel contained the sample to be dissolved and the external container the solvent consisting of 3 M sulfuric acid. Further details on the construction of the calorimeter and the experimental procedures are given in Lelet et al. (2011).

The low-temperature heat capacities of $CoSeO_3{\cdot}2H_2O$ and $NiSeO_3{\cdot}2H_2O$ was determined using adiabatic calorimetry from T = 8 to 340 K. Measurements were done using a ‘‘AK-9.02/BCT-21’’ calorimeter (Termax, Russia). The experimental precision was determined from the heat capacity measurements on synthetic corundum (mass fraction purity 0.99999) and benzoic acid (mass fraction purity 0.99998). The results show that with this calorimeter and the set-up used, $C_p^o(T)$ can be determined with a experimental precision of ±2% from T = 4 to 15 K, ±0.5% at T =

15 to 40 K and ±0.2% in the interval T = 40 to 340 K. The $C_p°$ results between 6 K and 300 K on benzoic acid relative to standard values (Gatta et al. 2006) are shown in Fig. 1. The agreement is better than ±0.2 % at T > 20 K and better than ±1.8 % at T < 20 K.

For the C_p^o determination of $CoSeO_3·2H_2O$ and $NiSeO_3·2H_2O$, 0.5271 and 0.7227 g of the samples were used. Liquid nitrogen and helium were used to obtain cryogenic temperatures in two different sets of measurements. One set of data was collected between T = (80 and 350) K and the other from T = 6 to 80 K. An evacuated ampoule containing a pellet of $CoSeO_3·2H_2O$ or $NiSeO_3·2H_2O$ was filled with dry helium to serve as a heat exchanger (room temperature and pressure 8 kPa). The ampoule was closed and hermetically sealed using indium. Further details on the construction of the calorimeter and the experimental procedures are given in (Varushchenko et al. 1997).

Results

Sample characterization

The obtained substances were in the form of small columnar, pink-violet (cobalt selenite) or green (nickel selenite) crystals of up to 10 μm in length and 0.5-2 μm wide. The X-ray powder diffraction data are shown in Fig. 2. The interplanar distances and the relative intensities of the peaks were derived by profile fitting using PDXL (version 2) software. They are in excellent agreement with data reported in PDF-2 entries 01-080-1391 (for cobaltomenite) and 9-009-364 (for ahfeldite). The unit cell parameters calculated from the powder data (table 1) are in good accordance with data obtained by other authors (Wildner, 1990; Vlaev et al, 2005, 2006). The X-ray fluorescence results gave a Co:Se ratio of 1.00:1.02 and Ni:Se ratio of 1.00:1.01. The amount of other elements was below the detection limit, which is approximately 0.003 wt% for all elements in the periodic chart from sodium to uranium. The infrared spectra are similar to those obtained by other authors (table 2). The combined use of these methods show that the synthetic products are single-phased, have the chemical composition $CoSeO_3·2H_2O$ or $NiSeO_3·2H_2O$.

Thus, the synthetic hydrous cobalt and nickel selenites correspond in structure and spectroscopic features to the natural cobaltomenite and ahlfeldite and may be used to determine its properties, in particular the thermodynamic parameters.

Enthalpy of formation

The determination of the standard enthalpy of formation, $\Delta_f H^o$(298 K), for $A^{II}SeO_3·2H_2O$ (A^{II}=Co, Ni) was performed using H_2SO_4-solution calorimetry. In order to do so, the enthalpy of solution at T = 298 K was determined for each of the following phases :

Na_2SeO_3(cr.) + (H_2SO_4 solution) → (solution A1) (1)

$A^{II}SO_4 \cdot 7H_2O$(cr.) + (solution A1) → (solution A2) (2)

$5H_2O$(l) + (H_2SO_4 solution) → (solution B1) (3)

Na_2SO_4(cr.) + (solution B1) → (solution B2) (4)

$A^{II}SeO_3 \cdot 2H_2O$(cr.) + (solution B2) → (solution B3) (5)

The respective values are given in table 3. Writing the reaction

$CoSO_4 \cdot 7H_2O$(cr.) + Na_2SeO_3(cr.) → $CoSeO_3 \cdot 2H_2O$(cr.) + Na_2SO_4(cr.) + $5H_2O$(l) (6)

and following Hess' law, one obtains:

$$\Delta_r H_6^o\ (298) = \Delta_r H_1^o\ (298) + \Delta_r H_2^o\ (298) - \Delta_r H_3^o\ (298) - \Delta_r H_4^o\ (298) - \Delta_r H_5^o\ (298) \quad (7)$$

And

$$\Delta_f H^o(298\ \text{K}, A^{II}SeO_3 \cdot 2H_2O, \text{cr.}) = \Delta_r H_7^o\ (298) + \Delta_f H^o(298\ \text{K}, A^{II}SO_4 \cdot 7H_2O, \text{cr.}) + \Delta_f H^o(298\ \text{K}, Na_2SeO_3, \text{cr.}) - \Delta_f H^o(298\ \text{K}, Na_2SO_4, \text{cr.}) - 5\,\Delta_f H^o(298\ \text{K}, H_2O, \text{l}) \quad (8)$$

From the experimental results in table 3 and from literature data (Wagman et al. 1982), namely $\Delta_f H^o$(298 K, $CoSO_4 \cdot 7H_2O$, cr.) = -2979.93 kJ/mol, $\Delta_f H^o$(298 K, $NiSO_4 \cdot 7H_2O$, cr.) = -2976.33 kJ/mol, $\Delta_f H^o$(298 K, Na_2SeO_3, cr.) = -958.6 kJ/mol, $\Delta_f H^o$(298 K, Na_2SO_4, cr.) = -1387.08 kJ/mol, $\Delta_f H^o$(298 K, H_2O, l) = -285.830 kJ/mol, one obtains $\Delta_f H^o$(298 K, $CoSeO_3 \cdot 2H_2O$, cr.) = -1135.3 kJ/mol, $\Delta_f H^o$(298 K, $NiSeO_3 \cdot 2H_2O$, cr.) = -1133.3 kJ/mol.

Heat-capacity behaviour

The raw low-temperature C_p^o data for $CoSeO_3 \cdot 2H_2O$ and $NiSeO_3 \cdot 2H_2O$ from both measurement series are given in tables 6 and 7. Fig. 3 shows a plot of the data. No obvious anomalies or phase transitions were observed. In order to extrapolate the heat-capacity down to T = 0 K, we used the equation $C_p^o = A \cdot T^n$, where A and n are fit parameters that were determined using experimental values between T = 8.70 and 11.75 for $CoSeO_3 \cdot 2H_2O$ and T = 9.18 and 14.85 for $NiSeO_3 \cdot 2H_2O$. In logarithmic form, one obtains $\ln C_p^o / \text{J} \cdot \text{mol}^{-1} \cdot \text{K}^{-1} = 0.8041 \cdot \ln(T/\text{K}) - 1.6023$ with a correlation coefficient of $R^2 = 0.9935$ for $CoSeO_3 \cdot 2H_2O$ and $\ln C_p^o / \text{J} \cdot \text{mol}^{-1} \cdot \text{K}^{-1} = 2.0596 \cdot \ln(T/\text{K}) - 4.8225$ with a correlation coefficient of $R^2 = 0.9838$ for $NiSeO_3 \cdot 2H_2O$. In standard notation one has $C_p^o = 0.2014 \cdot T^{0.8041}$ for $CoSeO_3 \cdot 2H_2O$ and $C_p^o = 0.00805 \cdot T^{2.0596}$ for $NiSeO_3 \cdot 2H_2O$.

The C_p^o data were fit with the polynomial (Dachs and Geiger 2006; Suleimanov et al. 2010):

$$C_p^o / \text{J} \cdot \text{mol}^{-1} \cdot \text{K}^{-1} = k_0 + k_1(T/\text{K})^{-3} + k_2(T/\text{K})^{-2} + k_3(T/\text{K})^{-0.5} + k_4(T/\text{K}) + k_5(T/\text{K})^2 + k_6(T/\text{K})^3 \quad (9)$$

Three separate temperature regions (from 8.1 to 15 K, 15 to 47 K, and 47 to 328 K for $CoSeO_3 \cdot 2H_2O$ from 9.2 to 16 K, 16 to 50 K, and 50 to 340 K for $NiSeO_3 \cdot 2H_2O$) were fit using nonlinear least-squares methods. The final least-squares best-fit values of the various *k* terms are

given in table 6. Fig. 4 shows the difference between experimental C_p^op values and fitted C_p^o values. Deviations are not more than 0.4% at T > 100 K and less than 5.6% at T < 100 K for $CoSeO_3 \cdot 2H_2O$ and 0.5% at T > 100 K and less than 8.3% at T < 100 K for $NiSeO_3 \cdot 2H_2O$.

Discussion

The standard third-law entropy, S^o, at T = 298.15 K was determined by solving the integral:

$$S^o = \int_{0K}^{298.15K} (C_p / T) dT \quad (10)$$

Values of S^o(298 K, $CoSeO_3 \cdot 2H_2O$, cr.) = 183.2 ± 1.0 J/(mol·K) and S^o(298 K, $NiSeO_3 \cdot 2H_2O$, cr.) = 172.9 ± 1.0 J/(mol·K) were obtained with an uncertainty of ±0.5%.

For the calculation of the entropy of formation, $\Delta_f S^o$ of $CoSeO_3 \cdot 2H_2O$ and $NiSeO_3 \cdot 2H_2O$ the experimentally measured third-law entropy S^o together with data from the literature were used by Dachs and Geiger (2006), that is S^o(298 K, Co, cr.) = 30.04 J/(mol·K), S^o(298 K, Ni, cr.) = 29.87 J/(mol·K), S^o(298 K, Se, cr.) = 42.442 J/(mol·K), S^o(298 K, O_2, gas.) = 205.138 J/(mol·K), S^o(298 K, H_2, gas.) = 130.684 J/(mol·K). One obtains $\Delta_f S^o$ (298 K, $CoSeO_3 \cdot 2H_2O$, cr.) = –(663.5 ± 1.0) J/(mol·K) and $\Delta_f S^o$ (298 K, $NiSeO_3 \cdot 2H_2O$, cr.) = –(673.6 ± 1.0) J/(mol·K).

The Gibbs energy of formation for $CoSeO_3 \cdot 2H_2O$ and $NiSeO_3 \cdot 2H_2O$ at T = 298 K, 1 atm. can be calculated based on the determined values of $\Delta_f H^o$ and $\Delta_f S^o$. We obtain $\Delta_f G^o$ (298 K, $CoSeO_3 \cdot 2H_2O$, cr.) = –937.4 J/(mol·K), $\Delta_f G^o$ (298 K, $NiSeO_3 \cdot 2H_2O$, cr.) = –932.4 J/(mol·K).

Selivanova et al. (1964) measured the heat of reaction between Na_2SeO_3 solution and $Co(NO_3)_2 \cdot 6H_2O$(cr.) and from this they calculated $\Delta_f H^o$ (298 K, $CoSeO_3 \cdot 2H_2O$, cr.) to be –1124.21 kJ/mol. The same authors (Selivanova et al. 1963) measured the heat of reaction between Na_2SeO_3 solution and $Ni(NO_3)_2 \cdot 6H_2O$(cr.) and obtained $\Delta_f H^o$ (298 K, $NiSeO_3 \cdot 2H_2O$, am.) to be -1121.73 kJ/mol. The difference between these values and our data is about 1%. It should be noted that although in the case of $NiSeO_3 \cdot 2H_2O$ the received value was obtained for an amorphous phase, it is very close to $\Delta_f H^o$ (298 K, $CoSeO_3 \cdot 2H_2O$, cr.) (Selivanova et al. 1964) (the difference is 2.5 kJ/mol, and the value for cobalt selenite there is less). For our data we observe the same relationship, as the value of $\Delta_f H^o$ (298 K, $CoSeO_3 \cdot 2H_2O$) is less by 2.0 kJ/mol than $\Delta_f H^o$ (298 K, $NiSeO_3 \cdot 2H_2O$). We suppose that both results of Selivanova et al. (1963; 1964) were obtained on amorphous phases.

The relevant results of our study are listed in tables 7, 8. Our value for S^o(298 K) is roughly 25% (for $CoSeO_3 \cdot 2H_2O$) and 14% (for $NiSeO_3 \cdot 2H_2O$) lower than given in Selivanova et al. (1963; 1964). Calculation of S^o(298 K, $CoSeO_3 \cdot 2H_2O$) (Selivanova et al. 1964) and S^o(298 K,

$NiSeO_3 \cdot 2H_2O$) (Selivanova et al. 1963) is performed by means of the $\Delta_f G^o$ values calculated from the data of Thukhlantsev and Tomashevsky (1957) on the solubility of cobalt and nickel selenites. The rather big difference between standard Gibbs energy and entropy of the formation of cobalt and nickel selenites is caused by a two order of magnitude's difference between the solubility products measured in Thukhlantsev and Tomashevsky (1957), viz. $((1.6\pm0.8)\cdot10^{-7}$ for $CoSeO_3$ and $(1\pm0.1)\cdot10^{-5}$ for $NiSeO_3$). The solubility of the salts was studied by Thukhlantsev and Tomashevsky (1957) without the identification of solid phases (by X-ray diffraction or by Schreinemakers's "rest" method) and without measurements of selenium concentration in the saturated solution. Therefore, we think our S^o(298 K) values, determined directly by low-temperature calorimetry, should be regarded as superior to those calculated from solubility data of Thukhlantsev and Tomashevsky (1957).

Based on the results of this investigation, table 9 contains smoothed $C_p°(T)$ values between T = 0 K and T = 320 K for $CoSeO_3 \cdot 2H_2O$ (cr.) and $NiSeO_3 \cdot 2H_2O$(cr.). Values for S^o and the functions $[H°(T)-H°(0)]$ and $[G°(T)-H°(0)]$ are also included.

Implications for Environmental Mineralogy

These results motivate a re-evaluation of the natural conditions under which selenites, and selenates replace selenides, and sulfides in the oxidation zones of sulfide ore deposits or upon weathering of technologic waste. Special attention should be given to a substantiation of the thermodynamic approach for modeling of mineral-forming processes in near-surface conditions.

The values of $\Delta_f G°$ for $CoSeO_3 \cdot 2H_2O$ and $NiSeO_3 \cdot 2H_2O$ were used to calculate the Eh–pH diagrams of the Co–Se–H_2O and Ni–Se–H_2O systems. Previously, these diagrams were calculated by Krivovichev et al. (2011), on the base of published data on solubility of $CoSeO_3 \cdot 2H_2O$ and $NiSeO_3 \cdot 2H_2O$ (Thukhlantsev and Tomashevsky, 1957). In this study, calculation and construction of Eh-pH diagrams were spent by means of software Geochemist's Workbench (GMB 7.0). The calculation of the diagrams was predated by the introduction of new data for $CoSeO_3 \cdot 2H_2O$ and $NiSeO_3 \cdot 2H_2O$ into the database and the specification of some constants. The activity coefficients are calculated from the Debye–Hückel equation. Eh-pH diagrams of Ni–Se–H_2O and Co–Se–H_2O systems have been constructed for the average contents of these elements in acidic waters of the oxidation zones of sulfide deposits (Krainov et al., 2004).

The Eh–pH diagram of the Co–Se–H_2O system (Fig. 5*a*) contains in addition to the stability field of native selenium, a stability field of Co_3O_4, which is unknown in nature, and the stability fields of CoSe (freboldite) and cobaltomenite formed in the neutral environment while Eh is not too high. The Eh–pH diagrams of the Ni–Se–H_2O system (Fig. 5*b*) contains the stability fields of

native selenium, $NiSe_2$ (penroseite) and Ni_3Se_4 (wilkmanite), and a wide field of NiO (bunsenite) and a field of ahlfeldite.

So, the behavior of selenium, the nearest geochemical counterpart of sulfur, in the surface environment can be quantitatively explained by variations of the redox potential and the acidity–basicity of the mineral-forming medium. Precisely these parameters determine the migration ability of selenium compounds and its precipitation in the form of various solid phases.

Acknowledgments

This work was supported by Saint-Petersburg State University grants (3.38.68.2011, and 3.38.83.2012) and DFG research foundation DE 412/40-1.

References

Charykova, M.V., Krivovichev, V.G., and Depmeier, W. (2010) Thermodynamics of arsenates, selenites, and sulfates in the oxidation zone of sulfide ores. II. Systems M_1, M_2 // $SO_4 - H_2O$ (M_1, M_2 = Fe^{2+}, Fe^{3+}, Cu^{2+}, Zn^{2+}, Pb^{2+}, Ni^{2+}, Co^{2+}, H^+) at 25°C. Geology of Ore Deposits, 52, 759–770.

Dachs, E., and Geiger, C.A. (2006) Heat capacities and vibrational entropies of mixing of pyrope-grossular ($Mg_3Al_2Si_3O_{12}$-$Ca_3Al_2Si_3O_{12}$) garnet solid solutions: A low temperature calorimetric and thermodynamic investigation. American Mineralogist, 91, 894–906.

Gatta, G.D., Richardson, M.J., Sarge, S.M., and Stølen, S. (2006) Standards, Calibration and Guidelines in MicroCalorimetry. Pure and Applied Chemistry , 78, 1455–1476.

Krainov, S.R., Ryzhenko, B.N., and Shvets, V.M. (2004) *Geokhimiya podzemnykh vod. Teoreticheskie, prikladnye i ekologicheskie aspekty* (Geochemistry of Subsurface Water: Theoretical, Applied, and Environmental Aspects), Moscow: Nauka (In Russian).

Krivovichev, V.G., Charykova, M.V., Yakovenko, O.S., Depmeier, W. (2011) Thermodynamics of Arsenates, Selenites, and Sulfates in the Oxidation Zone of Sulfide Ores. IV: Eh-pH diagrams of the Me-Se-H_2O systems (Me = Co, Ni, Fe, Cu, Zn, Pb) at 25°C. Geology of Ore Deposits, 53(7), 514–527.

Lelet, M.I., Sharkov, V.V., Nurgaliev, I.F., and Suleymanov, Ye.V. (2011) A new hardware solution in reaction calorimetry. Vestnik of Nizhny Novgorod State University, 3(1), 97-101.

Olin, A., Nolang, B., Osadchii, E.G., Ohman, L.-O., and Rosen, E. (2005) Chemical thermodynamics of Selenium. Amsterdam: Elsevier. 851 p.

Seby, F., Potin-Gautier, M., and Giffaut, E. (2001) A critical review of thermodynamic data for selenium species at 25 °C. Chemical Geology, 171, 173-194.

Selivanova, N.M., Leschinskaya, Z.L., Maier, A.I., Muzalev, E.Yu. (1964**)** Thermodynamic properties of cobalt selenite, $CoSeO_3 \cdot 2H_2O$. Izvestia Vuzov: Khimia i khimicheskaya tekhnologia, 7, 209-216 (In Russian).

Selivanova, N.M., Leshchinskaya, Z.L., Maier, A.I., Strel'tsov, I.S., Muzalev, E.Y. (1963) Thermodynamic properties of nickel selenite dehydrate. Russian Journal of Physical Chemistry, **37**, 837-839.

Suleimanov, E.V., Golubev, A.V., Alekseev, E.V., Geiger, C.A., Depmeier, W., and Krivovichev, V.G. (2010) A calorimetric and thermodynamic investigation of uranyl molybdate UO_2MoO_4. Journal of Chemical Thermodynamics, 42, 873–878

Thukhlantsev, V.G., and Tomashevsky, G.P. (1957) The solubility of the selenites of certain metals. Journal of the Analytical Chemistry of the USSR, 12, 303-309.

Treatise on Geochemistry. Vol. 9. Environmental geochemistry / Ed. B. S. Lonar (2004). Amsterdam: Elsevier Pergamon.

Varushchenko, R.M., Druzhinina, A.I., and Sorkin, E.L. (1997) Low-temperature heat capacity of 1-bromoperfluorooctane. The Journal of Chemical Thermodynamics, 29, 623–637.

Vlaev, L.T. , Genieva, S.D., and Gospodinov, G.G. (2005) Study of the crystallization fields of cobalt(II) selenites in the system $CoSeO_3$–SeO_2–H_2O. Thermal Analysis and Calorimetry, 81, 469-475.

Vlaev, L.T., Genieva, S.D., and Georgieva, V.G. (2006) Study of the crystallization fields of nickel(II) selenites in the system $NiSeO_3$–SeO_2–H_2O . Journal of Thermal Analysis and Calorimetry, 86, 449-456.

Wagman, D.D., Evans, W.H., Parker, V.B., Schumm, R.H., Halow, I., Bailey, S.M., Churney, K.L., and Nuttall, R.L. (1982) The NBS tables of chemical thermodynamic properties: Selected values for inorganic and C1 and C2 organic substances in (SI) units. Journal of Physical and Chemical Reference Data, 11, Supplement 2, 1-392.

Wildner, M. (1990) Crystal structure refinements of synthetic cobaltomenite ($CoSeO_3 \cdot 2H_2O$) and ahlfeldite ($NiSeO_3 \cdot 2H_2O$). Neues Jahrb. Mineral., Monatsh., 353–362.

TABLE 1. Cell parameters of $CoSeO_3 \cdot 2H_2O$ and $NiSeO_3 \cdot 2H_2O$.

Compound	$CoSeO_3 \cdot 2H_2O$			$NiSeO_3 \cdot 2H_2O$		
Space group	$P2_1/n$			$P2_1/n$		
a, Å	6.496 (1)	6.5322	6.494(6)	6.441 (2)	6.3782	6.442(9)
b, Å	8.809 (2)	8.8251	8.810(6)	8.746 (2)	8.7734	8.751(2)
c, Å	7.619 (2)	7.6455	7.614(4)	7.522 (3)	7.5467	7.521(0)
β, ^{0}	98.87 (1)	80.478	98.872(4)	99.00 (2)	81.451	99.008(1)
V, Å^3	430.74	434.67	430.493	418.54	417.61	418.828
	Wildner, 1990	Vlaev et al., 2005	This work	Wildner, 1990	Vlaev et al., 2006	This work
Formula units per cell	4			4		

TABLE 2**.** Infrared absorption spectra of $NiSeO_3 \cdot 2H_2O$ and $NiSeO_3 \cdot H_2O$

$CoSeO_3 \cdot 2H_2O$		$NiSeO_3 \cdot 2H_2O$		Band assignment
This work	Vlaev et al., 2005	This work	Vlaev et al., 2006	
492	492	501	500	$\delta_{(SeO3)2-}$
577	576	578	579	ν_{Co-O} (ν_{Ni-O})
697	700	703	700	$\nu_{as(SeO3)2-}$
792	790	799	800	$\nu_{s(SeO3)2-}$
813	815	842	841	$\nu_{s(SeO3)2-}$
			924	ρ_{H2O}
1507	1500	1527	1516	$\delta_{(OH)(H2O)}$
1613	1613	1624	1628	$\delta_{(OH)(H2O)}$
2938	2942	2916	2916	$\nu_{(OH)(H2O)}$
3130	3129	3118	3126	$\nu_{(OH)(H2O)}$
3220	3224	3197	3200	$\nu_{(OH)(H2O)}$
3429	3430	3452	3452	$\nu_{(OH)(H2O)}$

TABLE 3. Standard enthalpy of reactions (2) – (6), used for the calculation of $\Delta_f H^o$(298 K, $CoSeO_3 \cdot 2H_2O$, cr.) and $\Delta_f H^o$(298 K, $NiSeO_3 \cdot 2H_2O$, cr.)

№	Reaction (A^{II} - Co^{2+}. Ni^{2+})	$\Delta_r H°(298)$. (kJ/mol)	
		A^{II} - Co^{2+}	A^{II} - Ni^{2+}

1.	Na_2SeO_3(cr.) + (H_2SO_4 solution) → (solution A1)	-40.42 -41.36 -39.92 -40.07 -40.17 -39.97 -40.46 -41.77 -40.97	
		Mean -40.6 ± 0.5	
2.	$A^{II}SO_4 \cdot 7H_2O$(cr.) + (solution A1) → (solution A2)	36.00 36.75 36.14 35.72 34.62 35.56	34.58 34.40 34.06 34.94 34.86
		Mean 35.8 ± 0.7	Mean 34.57 ± 0.44
3.	$5H_2O$ + (H_2SO_4 solution) → (solution B1)	Mean 0	
4.	Na_2SO_4(cr.) + (solution B1) → (solution B2)	21.76 20.44 20.42 21.23 21.72 21.47	
		Mean 21.2 ± 0.6	
5.	$A^{II}SeO_3 \cdot 2H_2O$(cr.) + (solution B2) → (solution B3)	-12.84 -12.95 -13.32 -12.90 -12.93 -12.65 -12.54 -13.17 -13.07 -13.93 -12.69 -12.89	-13.09 -12.43 -12.34 -12.86 -12.65
		Mean -13.0 ± 0.2	Mean -12.67 ± 0.38

TABLE 4. Raw low-temperature heat capacity, $C_p°$ (J/(mol·K)), data for $CoSeO_3 \cdot 2H_2O$ (cr., M=221.922g/mol).

T (K)	Cp°	T (K)	Cp°	T (K)	Cp°	T (K)	Cp°	T (K)	Cp°
Series 1		18.5	2.858	56.8	34.94	105.4	80.01	196.8	134.7
8.1	1.134	18.8	2.943	57.8	35.95	107.4	81.62	198.9	135.8

8.3	1.132	19.0	3.05	58.7	36.89	109.4	83.20	201.5	136.9
8.4	1.134	19.3	3.14	59.6	37.89	111.4	84.65	204.5	138.0
8.6	1.138	19.6	3.24	60.6	38.92	113.4	86.09	207.6	139.3
8.7	1.160	19.9	3.37	60.5	38.72	115.4	87.56	210.6	140.7
8.8	1.174	20.5	3.58	61.4	39.69	117.4	88.98	213.7	142.2
9.0	1.178	21.3	3.93	62.8	41.13	119.4	90.48	216.7	143.5
9.1	1.192	22.2	4.30	63.3	41.64	121.4	91.80	219.8	144.8
9.3	1.200	23.1	4.69	64.0	42.34	123.4	93.27	222.8	146.1
9.4	1.218	23.9	5.07	64.7	43.10	125.4	94.62	225.9	147.7
9.5	1.229	24.2	5.30	65.2	43.56	127.4	96.01	228.9	149.0
9.7	1.243	25.1	5.77	66.7	45.06	129.5	97.24	232.0	150.1
9.8	1.257	26.0	6.28	67.9	46.28	131.5	98.52	235.0	151.5
10.0	1.278	26.9	6.81	68.7	47.11	133.5	99.79	238.1	151.6
10.2	1.300	27.8	7.38	69.9	48.24	135.6	101.3	241.1	153.7
10.4	1.315	28.7	7.99	70.7	49.00	137.6	102.5	244.1	155.4
10.7	1.347	29.6	8.62	71.6	49.88	139.6	103.8	247.2	156.7
11.0	1.375	30.5	9.29	72.6	50.84	141.6	105.0	250.2	158.4
11.2	1.409	31.5	9.98	73.7	51.84	143.7	106.3	253.2	159.0
11.5	1.445	32.4	10.71	74.5	52.61	145.7	107.5	256.3	160.1
11.8	1.476	33.3	11.46	75.5	53.51	147.7	108.8	259.3	161.4
12.0	1.517	34.3	12.25	76.9	54.82	149.8	109.9	262.3	162.7
12.3	1.558	35.3	13.08	77.5	55.33	151.8	111.0	265.3	164.0
12.6	1.595	36.2	13.91	78.3	56.09	153.9	112.4	268.3	165.0
12.8	1.621	37.2	14.71	79.4	57.03	155.9	113.6	271.3	166.1
13.1	1.660	38.5	16.04	80.4	57.95	157.9	114.7	274.3	167.2
13.4	1.702	39.4	16.99	81.4	59.43	160.0	115.8	277.2	168.4
13.7	1.748	40.4	17.82	82.5	60.77	162.0	117.0	280.2	169.5
13.9	1.791	41.4	18.86	83.4	61.76	164.1	118.1	283.2	170.5
14.2	1.832	42.4	19.82	84.8	63.05	166.1	119.1	286.2	171.6
14.5	1.886	43.4	20.66	86.3	64.28	168.2	120.6	289.1	172.7
14.8	1.936	44.3	21.74	87.8	65.57	170.2	121.4	292.1	173.6
15.1	1.988	45.3	22.67	89.3	67.00	172.3	122.5	295.0	174.8
15.3	2.049	46.3	23.64	90.8	68.17	174.3	123.6	297.9	176.4
15.6	2.107	47.3	24.70	92.3	69.38	176.4	124.7	301.3	177.9
15.9	2.168	48.2	25.85	93.8	70.55	178.4	125.7	305.2	178.7
16.2	2.242	49.2	26.87	95.3	71.78	180.5	126.7	309.1	179.9
16.5	2.314	50.2	27.88			182.5	127.9	313.0	181.1
16.7	2.381	51.1	28.86	***Series 2***		184.6	129.0	316.8	182.4
17.0	2.444	52.1	29.85	96.7	73.10	186.6	129.9	320.6	183.6
17.3	2.523	53.1	30.89	98.2	74.25	188.7	130.9	324.4	184.9
17.6	2.599	54.0	31.91	99.7	75.29	190.7	131.8	328.2	186.1
17.9	2.687	55.0	32.93	101.4	77.13	192.8	132.9		
18.2	2.788	55.9	33.94	103.4	78.63	194.8	134.1		

340
341

TABLE 5. Raw low-temperature heat capacity, $C_p°$ (J/(mol·K)), data for $NiSeO_3·2H_2O$ (cr., M=221.68 g/mol).

T (K)	Cp°	T (K)	Cp°	T (K)	Cp°	T (K)	Cp°	T (K)	Cp°
Series 1		19.5	3.770	56.6	31.227	93.0	63.731	201.8	133.012
9.2	0.728	19.8	3.880	57.6	32.084	95.0	65.563	205.9	135.072
9.5	0.872	20.1	4.021	58.6	33.056	96.9	67.540	210.0	137.109
9.8	0.883	20.7	4.342	59.7	35.035	98.9	69.610	214.0	139.153
10.0	1.005	21.6	4.670	60.7	35.968	100.9	70.902	218.2	141.444
10.3	0.950	22.4	5.081	61.7	36.815	103.4	72.060	222.3	143.041
10.6	1.093	24.6	6.245	62.8	36.784	109.3	76.141	226.3	144.941
10.9	1.069	25.9	6.865	63.8	38.288	112.3	78.299	230.4	146.871
11.2	1.110	26.7	7.214	64.8	39.000	115.7	80.558	234.5	148.806
11.4	1.175	27.6	7.459	65.9	40.124	119.1	82.838	238.6	150.591
11.7	1.331	28.7	8.159	66.9	40.641	122.1	85.052	242.6	152.460
12.0	1.334	30.1	8.810	67.9	42.266	125.1	87.123	246.7	154.283
12.3	1.403	31.2	9.406	69.0	42.878	128.1	89.179	250.8	155.950
12.6	1.447	32.2	9.691	70.1	44.024	131.2	91.200	254.9	157.793
12.8	1.433	33.1	10.786	71.6	45.406	134.2	93.261	258.9	159.207
13.1	1.620	34.1	11.686	73.6	47.343	137.2	95.225	263.0	161.071
13.7	1.819	35.1	12.265	75.7	48.559	140.2	97.193	267.0	162.737
14.0	1.852	36.1	13.039	77.7	50.451	143.3	99.105	271.1	164.221
14.3	1.936	37.1	13.581	78.6	51.636	146.3	101.115	275.1	165.926
14.6	2.003	38.0	13.972			149.4	103.047	279.2	167.483
14.8	2.137	39.0	14.803	***Series 2***		152.4	104.810	283.2	169.542
15.1	2.392	40.0	15.896	66.9	40.641	155.5	106.676	287.3	170.628
15.4	2.298	41.0	17.244	67.9	42.266	158.5	108.581	291.3	171.893
15.7	2.494	42.0	18.190	69.0	42.878	161.6	110.449	295.3	173.414
16.0	2.479	43.0	19.271	70.1	44.024	164.6	112.337	299.3	174.750
16.3	2.536	44.0	19.740	71.6	45.406	167.7	114.064	303.9	177.278
16.6	2.686	45.0	19.994	73.6	47.343	170.8	115.879	309.2	178.302
16.9	2.791	46.0	20.868	75.7	48.559	173.8	117.561	314.5	179.787
17.2	2.892	47.0	22.517	77.7	50.451	176.9	119.299	319.7	181.712
17.5	2.993	48.1	23.229	78.6	51.636	179.9	120.968	324.8	183.555
17.8	3.011	49.1	24.145	80.9	53.749	183.0	122.645	329.9	185.638
18.0	3.097	50.1	24.898	83.0	55.407	186.0	124.317	335.0	187.732
18.3	3.315	52.3	27.270	85.0	57.030	189.1	125.994	340.0	189.609
18.6	3.334	53.5	28.300	87.0	58.626	192.2	127.689		
18.9	3.541	54.6	29.307	89.0	60.315	195.2	129.309		
19.2	3.594	55.6	30.403	91.0	61.972	198.3	130.914		

TABLE 6. Best-fit coefficients for use in the $C_p°$ polynomial in eq. (10) for three temperature intervals.

T (K)		k_0	k_1	k_2	k_3	k_4	k_5	k_6
A^{II}-Co^{2+}	8.1-15	-7955.14	215203	-97861.6	19422.8	355.448	-11.359	0.159242
	15-47	367.663	-94097.8	20223	-1295.14	-8.10942	0.138739	-0.000847
	47-328	442.7	$-7.431\cdot10^{6}$	441169	-3561.84	-0.66795	0.002145	$-2.137\cdot10^{-6}$
A^{II}-Ni^{2+}	9.2-16	0.101264	-	-	-	-0.04141	$-7.48\cdot10^{-4}$	0.0004854
	16-50	50.5953	343758	-44773.1	468.12	-7.0692	0.17244	-0.001236
	50-340	-292.949	$1.2469\cdot10^{7}$	-534922	2445.99	1.90914	-0.00352	$2.833\cdot10^{-6}$

TABLE 7. Comparison of thermodynamic functions for $CoSeO_3\cdot2H_2O$ (cr.).

Reference	$C_p°$(298.15 K) (J/(mol·K))	$S°$(298.15 K) (J/(mol·K))	$\Delta_fH°$(298 K) (kJ/mol)	$\Delta_fG°$(298.15 K) (kJ/mol)
This work	176.6 ± 1.0	183.2 ± 1.0	-1135.3 ± 2.3	-937.4 ± 2.5
N.M. Selivanova et al. (1964)	-	228.6 (cr.)*	-1124.21 (cr.)	-940.6(cr.)*

*calculated using the data on solubility of $CoSeO_3\cdot2H_2O$ (Thukhlantsev and Tomashevsky, 1957)

TABLE 8. Comparison of thermodynamic functions for $NiSeO_3\cdot2H_2O$ (cr.).

Reference	$C_p°$(298.15 K) (J/(mol·K))	$S°$(298.15 K) (J/(mol·K))	$\Delta_fH°$(298 K) (kJ/mol)	$\Delta_fG°$(298.15 K) (kJ/mol)
This work	174.3 ± 1.0	172.9 ± 1.0	-1133.3 ± 2.2	-932.4 ± 2.5
N.M. Selivanova et al. (1963)	-	196.8 (am.)*	-1121.73 (am.)	-928.0(cr.)*

*calculated using the data on solubility of $NiSeO_3\cdot2H_2O$ (Thukhlantsev and Tomashevsky, 1957)

TABLE 9. Smoothed values for the thermodynamic functions of $A^{II}SeO_3 \cdot 2H_2O$ ($A^{II} – Co^{2+}$. Ni^{2+}).

T	$C_p°$		$H°(T)-H°(0)$		$S°(T)$		$-[G°(T)-H°(0)]$	
	A^{II} - Co^{2+}	A^{II} - Ni^{2+}	A^{II} - Co^{2+}	A^{II} - Ni^{2+}	A^{II} - Co^{2+}	A^{II} - Ni^{2+}	A^{II} - Co^{2+}	A^{II} - Ni^{2+}
[0]	[0]	[0]	[0]	[0]	[0]	[0]	[0]	[0]
20	3.409	3.982	0.02919	0.02052	2.491	1.328	0.02064	0.006044
40	17.44	15.9	0.2174	0.2051	8.463	7.275	0.1211	0.0859
60	38.21	35.39	0.7716	0.7082	19.41	17.22	0.3931	0.3252
80	57.52	53.04	1.736	1.58	33.15	29.63	0.9159	0.7904
100	75.57	70.41	3.081	2.807	48.09	43.25	1.727	1.518
120	90.89	83.5	4.752	4.34	63.27	57.19	2.841	2.522
140	104	97.07	6.703	6.148	78.29	71.1	4.257	3.805
160	115.8	109.5	8.904	8.215	92.96	84.88	5.97	5.365
180	126.5	121	11.33	10.52	107.2	98.45	7.973	7.199
200	136.4	131.9	13.96	13.05	121.1	111.8	10.26	9.302
220	144.8	142.2	16.77	15.79	134.5	124.8	12.81	11.67
240	152.8	151.2	19.75	18.73	147.4	137.6	15.63	14.29
260	161.7	159.7	22.91	21.84	160.1	150	18.71	17.17
273.15	166.8	165.1	25.07	23.98	168.2	158.1	20.87	19.2
280	169.5	167.9	26.22	25.12	172.3	162.2	22.03	20.29
298.15	176.6	174.3	29.35	28.23	183.2	172.9	25.26	23.33
300	177.4	175.1	29.68	28.55	184.3	174	25.6	23.65
320	183.4	181.8	33.29	32.12	195.9	185.5	29.4	27.25

T (K); $C_p°$ (J/(mol·K)); $H°(T)-H°(0)$ (kJ/mol);
$S°(T)$ (J/(mol·K)); $-[G°(T)-H°(0)]$ (kJ/mol)

374 **Figure Captions**
375

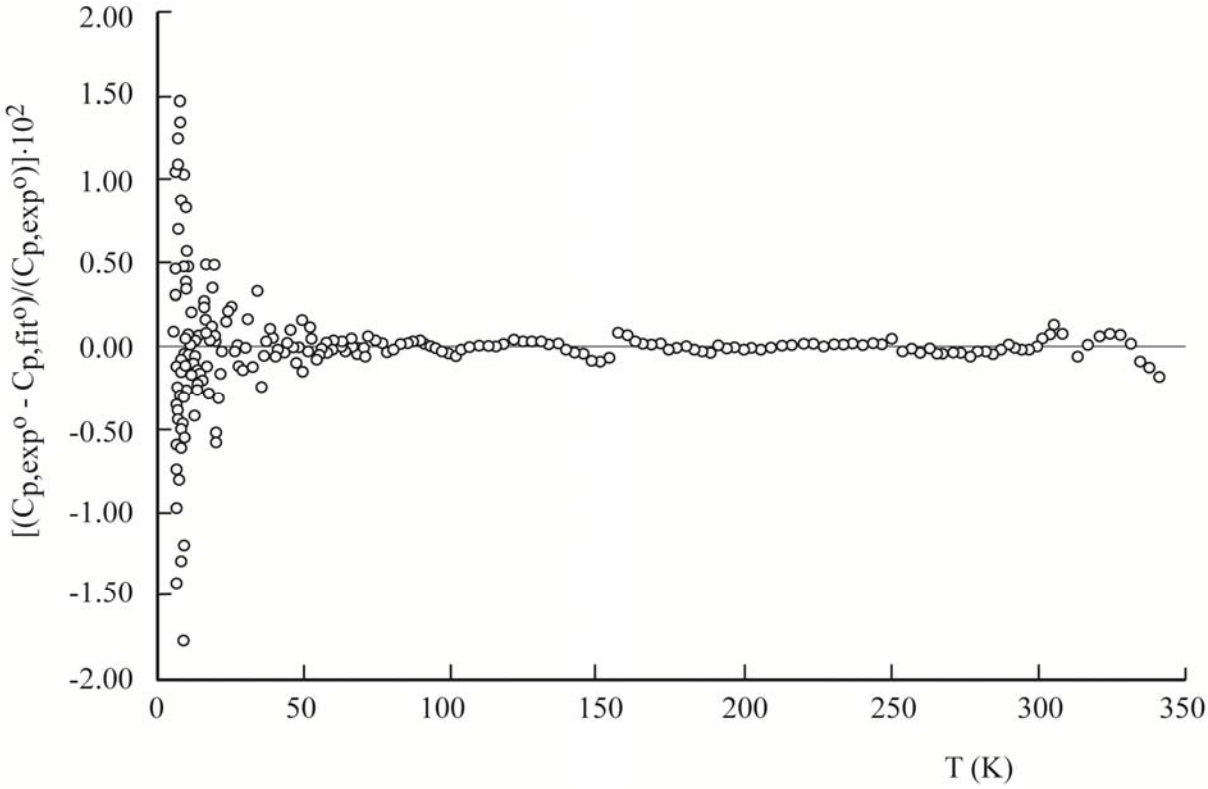

376
377
378 Figure 1. Deviations of experimental $C_p°$ on benzoic acid from (Gatta et al 2006).
379
380
381

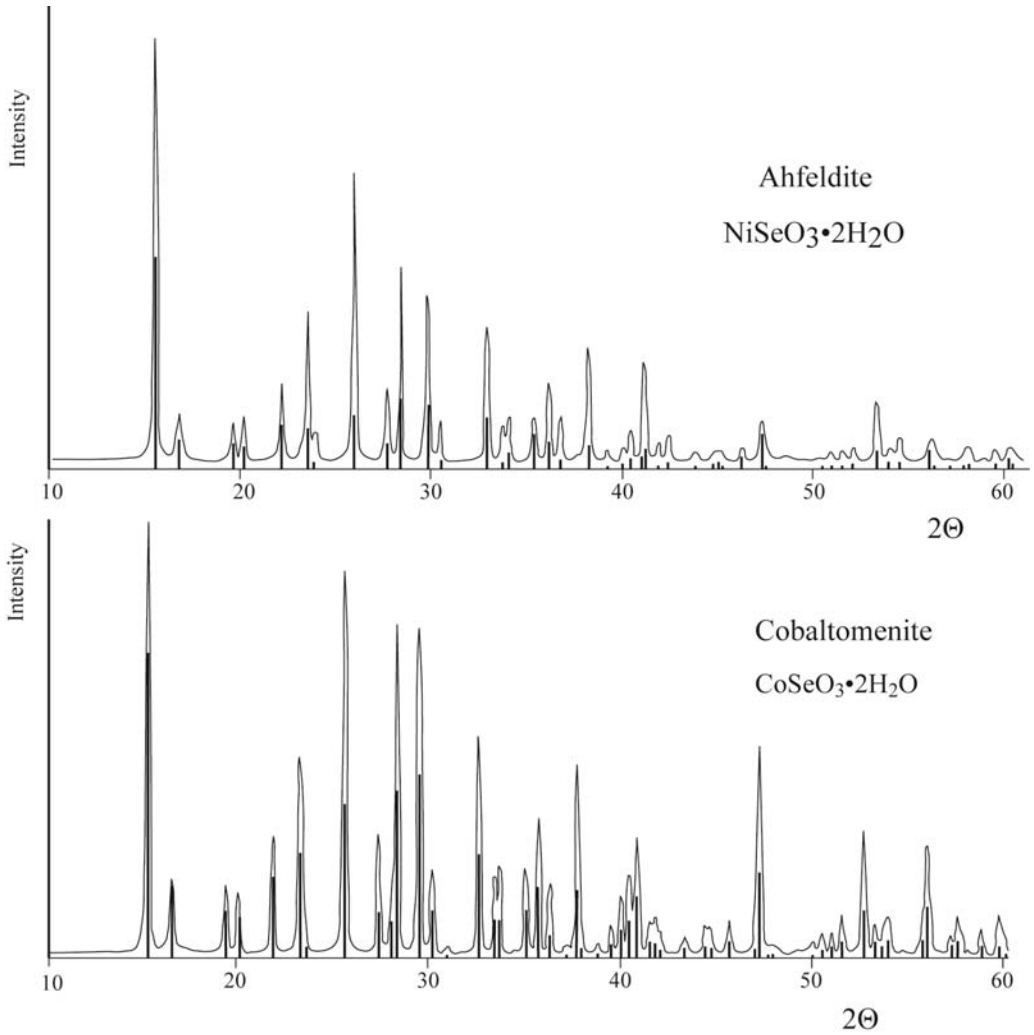

382

383 FIGURE 2. X-ray powder diffraction diagram of $CoSeO_3 \cdot 2H_2O$ and $NiSeO_3 \cdot 2H_2O$ (curve lines are
384 experimental results, black vertical lines are PDF-2 entries 01-080-1391 (for cobaltomenite) and 9-
385 009-364 (for ahfeldite)).

386
387
388
389
390

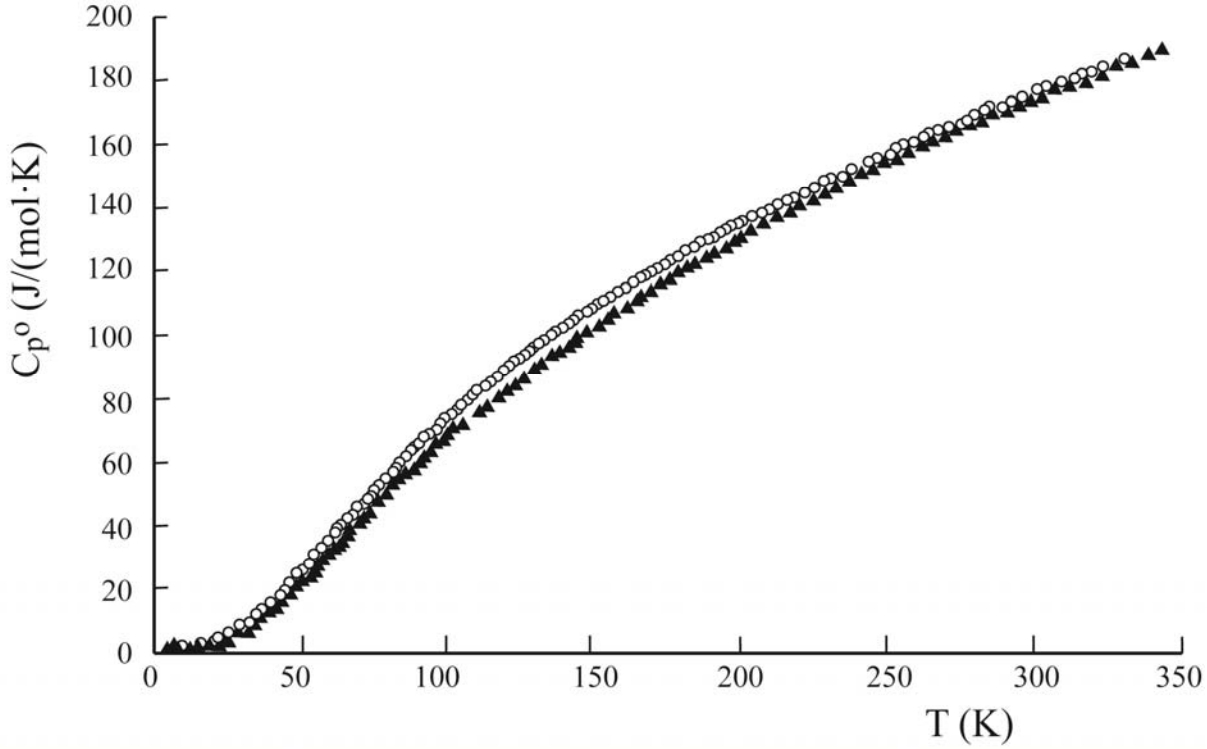

FIGURE 3. Plot of our experimental low-temperature $C_p°$ results for against temperature between T = (8 and 328) K for $CoSeO_3·2H_2O$ and T = (10 and 340) K for $NiSeO_3·2H_2O$. Data for $CoSeO_3·2H_2O$ are shown as rings and those for $NiSeO_3·2H_2O$ as solid triangles.

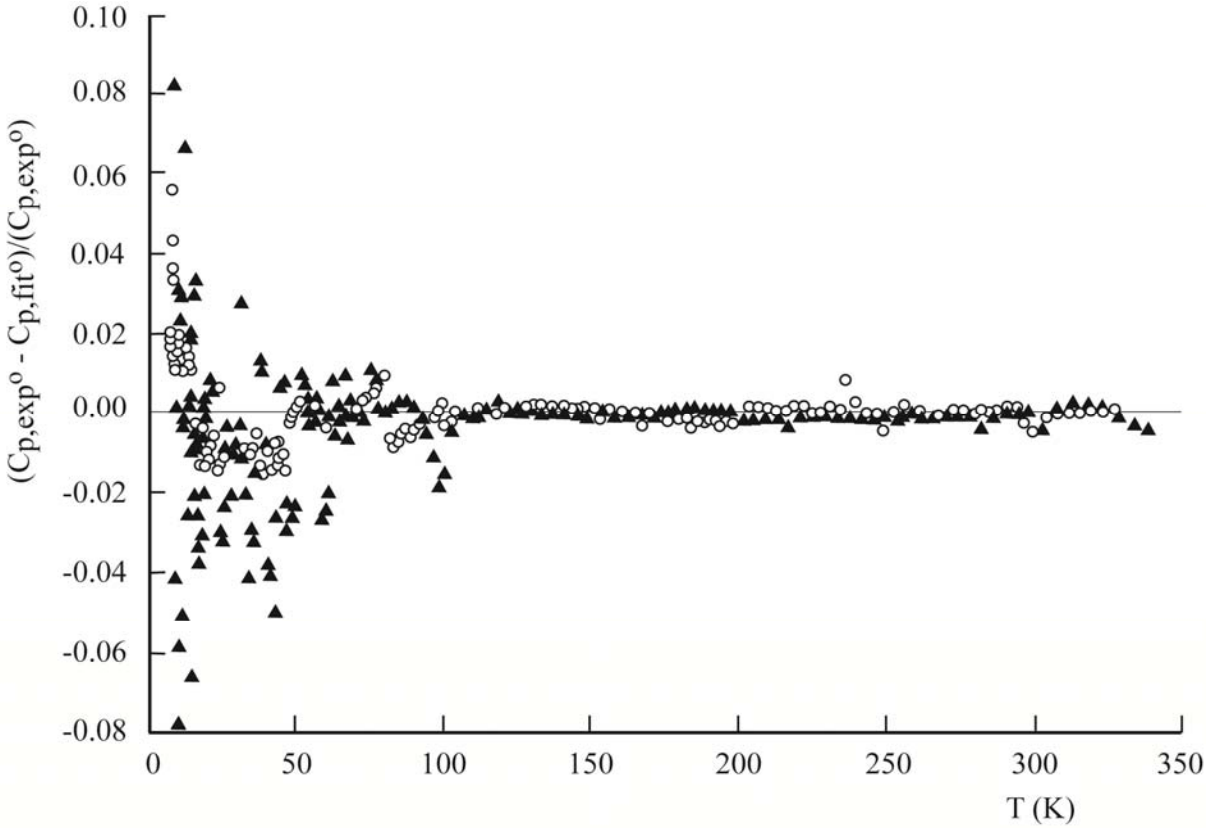

FIGURE 4. Plot of heat capacity against temperature to illustrate the deviation of the experimental low-temperature $C_p°$ values from the polynomial fit (Eq. (10) and (table 6). Data for $CoSeO_3 \cdot 2H_2O$ are shown as rings and those for $NiSeO_3 \cdot 2H_2O$ as solid triangles.

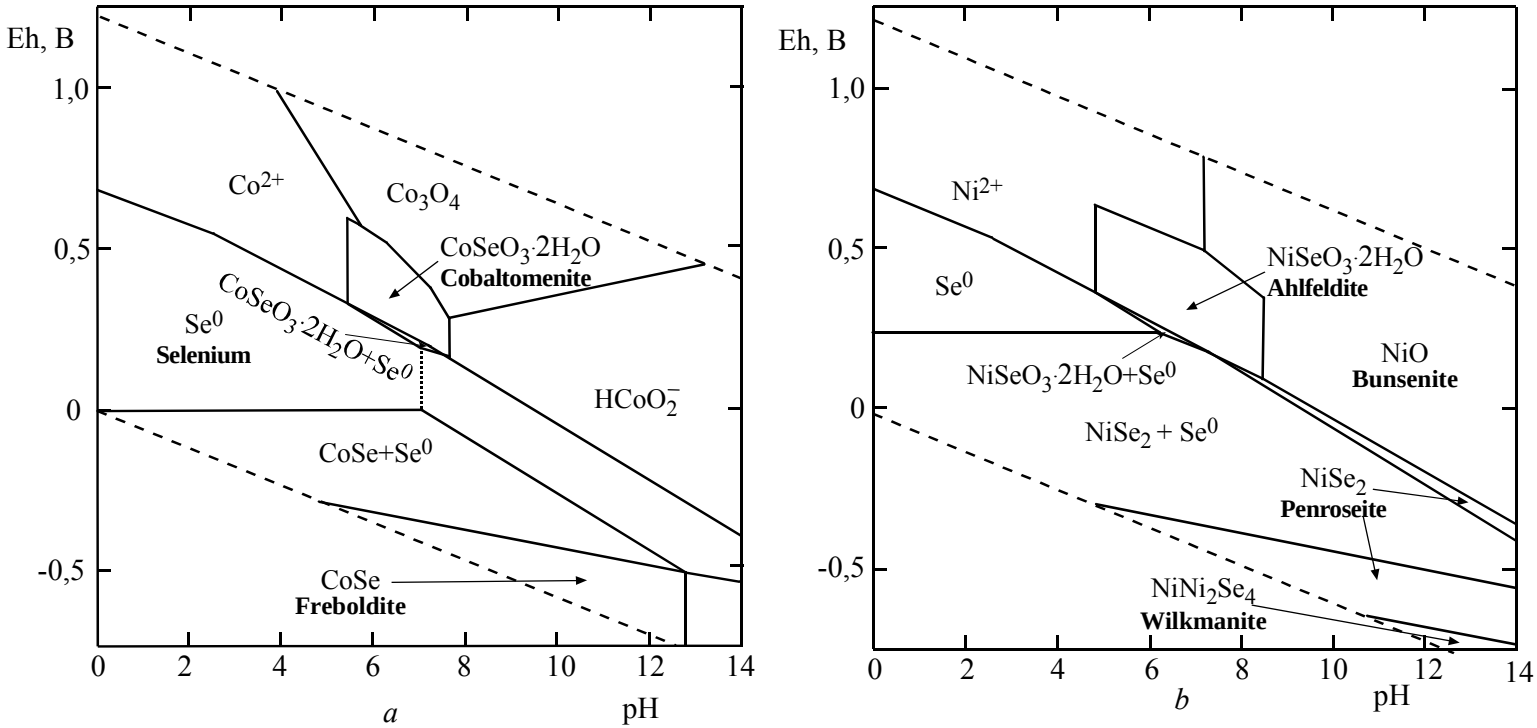

FIGURE 5. Eh–pH diagrams of the Co–Se–H_2O (*a*) and Ni–Se–H_2O (*b*) systems at 25°C. The activities of the components: (*a*) $a_{\Sigma Se} = 10^{-3}$, $a_{\Sigma Co} = 10^{-2}$ and (*b*) $a_{\Sigma Se} = 10^{-3}$, $a_{\Sigma Ni} = 10^{-2}$.